CloudSat Project

A NASA Earth System Science Pathfinder Mission

CloudSat 2C-PRECIP-COLUMN Data Product Process Description and Interface Control Document

Product Version: P1_R05
Document Revision: 1
Date: 26 January 2018

Questions concerning the document and proposed changes shall be addressed to

    John M. Haynes
    john.haynes@colostate.edu
    (970) 491-8535

Document Revision History

Date	Revision	Description	Section(s) Affected
31 March 2017	0	Initial Release	All
26 January 2018	1	Added variables	1.1, 5.3, 6

Contents

1 Introduction

This document provides an overview of the 2C-PRECIP-COLUMN precipitation algorithm for CloudSat. The objective of the algorithm is to identify surface precipitation and quantify its characteristics based on CloudSat Profiling Radar (CPR) observations. This product now primarily focuses on precipitation incidence and quantification of path integrated attenuation; most users are directed to the 2C-RAIN-PROFILE product for rain rate information. That product considers the full radar reflectivity profile and allows precipitation rate to vary with height (unlike this product, which provides a "column" estimate). Even so, the present product features a mature precipitation algorithm that continues to be maintained and updated, and as a service to users the precipitation rate variables have been retained, but renamed. 2C-RAIN-PROFILE and 2C-SNOW utilize the precipitation incidence from the present product.

The algorithm makes use of the radar reflectivity near the surface of the earth and an estimate of path integrated attenuation (PIA) determined from the surface reflection characteristics to determine precipitation incidence and intensity (though intensity is only reported over open-water surfaces). The remainder of this document describes the algorithm in greater detail. Section 2 provides an overview of the theoretical basis upon which the algorithm is built. Sections 3 and 4 describe inputs to the algorithm and detail its implementation. The output format for the product is summarized in Section 5, an example shown in Section 6, and instructions for the operator can be found in Section 7.

1.1 What's New: Product Version History

Changes in version P1_R05 include:

− PIA and its uncertainty as determined using the wind speed/SST method are now reported regardless of whether they are used in the retrieval ($Diagnostic\_PIA\_hydrometeor\_ws$ and $Diagnostic\_PIA\_uncertainty\_ws$).

Changes in version P_R05 include:

− This product now primarily focuses on precipitation incidence; for more details read the Introduction above. A side effect is that some variables have been renamed; $Precip\_rate$ becomes $Diagnostic\_precip\_rate$, and so on.
− The convective and stratiform retrievals have been rebuilt from the ground-up, and now share a largely unified code base. New lookup tables of precipitation rate and path integrated attenuation have been built using Robin Hogan's Time-Dependent Two-Stream model of multiple scattering (Hogan and Battaglia 2008). Improvements have also been made that should result in better simulation of the CloudSat radar's antenna beam pattern.
− A new method of determining PIA, using local observations of the clear sky surface, is used when available. This significantly reduces uncertainty in PIA, especially over the ocean surface (see Section 2.1.1).
− PIA is now reported everywhere it can be calculated, including for non-raining profiles. It is reported (experimentally) over non-water surfaces.
− Various bug fixes.

Changes in version P2_R04 include:

− AMSR-E based sea ice detection has been replaced with the daily sea ice product from SSM/I as found in the CloudSat CRYOSPHERE-AUX product (see Section 3.2.2). This provides a near-operational, 'bigger picture' of the sea ice coverage surrounding the CloudSat track, and therefore improves the precipitation retrievals. The variable $Surface\_type$ has changed accordingly.
− Numerous data gaps in the 2C-PRECIP-COLUMN produced by AMSR-E data outages are now eliminated.
− Various bug fixes.

Changes in version P1_R04 include:

− The precipitation incidence flag is now produced over land, ocean, and sea ice (although quantitative precipitation rate retrievals are only performed over ocean).
− A convective/stratiform flag has been added.
− For profiles that are determined to be convective, a new retrieval pathway is followed that considers supercooled water lofted above the melting level in convective cores.
− The clear-sky surface backscatter calculations have been improved, and a correction is now applied to this quantity by requiring CloudSat-identified cloud layers to be saturated with respect to liquid.
− Some variables have been renamed, in part to discourage their use except as diagnostics. In particular, $Retrieval\_info\_flag$ becomes $Diagnostic\_retrieval\_info$, $Phase\_flag$ becomes $Diagnostic\_retrieval\_type$, and SRT_flag becomes $Diagnostic\_SRT$.
− $Precip\_flag$ is now more clearly separated by precipitation type at the surface. In particular, profiles that may contain frozen precipitation are now segregated as snow or mixed. The snow profiles are highly likely to actually contain be entirely snow at the surface, whereas the mixed profiles may contain (or be) rain.
− The AMSR-E products are no longer passed through 2C-PRECIP-COLUMN. These products are now available in their own AMSR-AUX product.

2 Algorithm Theoretical Basis

The physical basis of the retrieval is outlined in Haynes et al. (2009), and quantitative and physical details of the retrieval may be obtained from this source. Updates to the algorithm since the publication of Haynes et al. (2009) are highlighted in Section 2.1.

In summary, this algorithm utilizes measurements of hydrometeor path integrated attenuation (PIA) to retrieve precipitation rate. The PIA, which may be derived using radar measurements of the strength of the backscatter from the earth's surface, is directly related to the precipitation rate in the overlying atmosphere. This algorithm makes the simplifying assumption that precipitation rate is constant with height.

Multiple scattering within the precipitating column can be significant for rainfall exceeding a few millimeter per hour (Battaglia et al. 2007), so a forward model of multiple scattering (Hogan and Battaglia 2008) is used to simulate the relationship between rainfall and observed PIA for

various vertical profiles of precipitation. This results in a number of lookup tables related to factors like cloud depth and freezing level height, and the tables are used to retrieve precipitation rate.

For profiles determined to be stratiform, a model of the melting layer is incorporated into the multiple scattering calculations to better represent the transition from snow to rain. This melting layer model aims to treat the attenuating characteristics of melting snowflakes. The model follows snow (modeled through the discrete dipole approximation) falling through a melting layer and melting into rain, assuming a constant lapse rate, Γ_e, of 6 °C km^{-1}. Liquid or mixed precipitation layers are considered to extend to the height of the lowest continuous cloud layer, H_{CTL}, as determined from the 2B-GEOPROF cloud mask, capped by the height of the freezing level, H_f, from ECMWF-AUX. The effects of purely frozen precipitation on PIA are only considered when a core of 10 dBZ of greater reflectivity extends through the freezing level, H_{sig}. When such a core is absent, melting is considered to start at the freezing level itself.

For profiles determined to be convective or shallow, in addition to H_f and H_{sig}, the rain top height H_{RT} is also evaluated for the profile. Precipitation is considered completely frozen between H_{RT} and H_{sig}. It is taken to be a mix of frozen precipitation and supercooled water between H_f and H_{RT}, the fractional ice component being a linear function of distance between the two limits. Although this treatment neglects the preferential growth of ice particles as dictated by the Bergeron-Findeisen process (Wallace and Hobbs 2006), it is likely to be a considerably better approximation than the gradual melting of ice particles considered by the stratiform portion of the retrieval. Precipitation below H_f is taken to be liquid, and once again precipitation cannot extend higher than H_{CTL}.

The unattenuated radar reflectivity, Z_u, near the surface is closely related to the presence of rain; the higher Z_u the more likely precipitation is occurring. Z_u is the sum of the measured near-surface reflectivity Z_{ns}, the PIA (scaled to be applicable at the near-surface height, using the retrieved precipitation rate if available), and a component due to gaseous attenuation, G (determined from the ECMWF-AUX temperature and moisture profile).

2.1 Algorithm Updates and Additional Notes

2.1.1 Determination of Path Integrated Attenuation

One of two methods is used to determine the PIA. The first method of determining PIA depends on the well-behaved relationship between the backscatter cross section of the ocean surface, σ_0, and the wind speed, V, at the ocean surface. Higher wind speeds cause greater roughening of the ocean surface, resulting in increased scattering of microwave radiation away from the radar receiver and a lower resulting surface backscatter cross section. The sea surface temperature (SST) also influences the backscatter cross section through variation of the index of refraction. A database of observations of the surface backscatter cross section under clear-sky conditions, σ_{clr}, provides a background reference for the state of the surface when hydrometeors are absent. When cloud or rain is present, the observed backscatter cross section is reduced by hydrometeor attenuation. This reduction allows calculation of PIA given knowledge of the wind speed at the ocean surface (derived from a numerical model) and, to a lesser extent, the SST (Li et al. 2005).

The second method of determining PIA is the "interpolation method" whereby σ_{clr} is obtained by searching thirty profiles surrounding the profile of interest for profiles where the sky is determined to be clear, and then taking a weighted mean of the observed values of σ_0 for those profiles.

In particular, if n clear profiles are located, then

$$\sigma_{clr} = \frac{\sum_{i=1}^{n} w_i \cdot \sigma_{0,i}}{\sum_{i=1}^{n} w_i} , \tag{1}$$

where $w_i = \exp(-D_i/f)$, D is the distance to the clear sky profile, and f is a scaling factor (set to 5 km). PIA then follows from as the difference between the clear sky and observed σ_0. This method is only used if a certain number of clear-sky profiles are available ($n = 5$), and the surface type is uniform. It is therefore likely to fail in the case of extensive, unbroken clouds decks, and the first method of calculating PIA is utilized instead in this case.

During the retrieval process, an attempt is always made to use the interpolation method first since uncertainties are generally lower. If this fails, the wind speed/SST method is used. Where PIA can be determined, the variable $Diagnostic\_PIA\_Method$ indicates which method was used. Over land, only the interpolation method is available. PIA determination over non-open water surfaces is considered highly uncertain: the variables $Experimental\_land\_PIA$ and $Experimental\_land\_PIA\_uncertainty$ contain this information but should be considered experimental and not used without first consulting a member of the CloudSat precipitation team (see cover page).

2.1.2   Convective/Stratiform Determination

Each rain certain pixel is identified as being convective, stratiform, or shallow based on the vertical structure of reflectivity. The principle that liquid precipitation causes significant attenuation of the W-band radar reflectivity profile is central to the approach. Strong updrafts in convective precipitation lift significant amounts of liquid water above the 0°C freezing level while stratiform precipitation is characterized by primarily frozen hydrometeors above the freezing level, a well-defined melting layer approximately 500 m below the freezing level, and liquid precipitation below that.

Thus convective and stratiform precipitation can be distinguished by examining the height at which attenuation becomes evident in the reflectivity profiles. Convective profiles, like those shown in the top three rows of Figure 1, are characterized by reflectivity profiles that increase with height from the surface to well above the freezing level while stratiform reflectivity profiles (bottom 2 rows of figure) exhibit an inflection point near the freezing level corresponding to the melting layer. In 2C-PRECIP-COLUMN the height of this inflection point is assumed to represent the top of the liquid precipitation in the column. If this height is more than 500 m above the ECMWF 0°C level then the pixel is flagged as convective, otherwise it is identified as being stratiform. In the absence of a reflectivity value of 0 dBZ or greater above the freezing level, the pixel is classified as shallow. 2C-PRECIP-COLUMN reports both the rain type assigned to each pixel as well as the estimated top of the liquid precipitation column.

2.1.3   Identification of Sea Ice

The presence of sea ice precludes the use of the wind speed/SST method of determining PIA, so it is important to know if sea ice is present in a given profile. Sea ice (and inland lake ice) is identified using ice products from SSM/I (Special Sensor Microwave Imager/Sounder) produced by the National Snow and Ice Data Center (Nolin et al. 1998). To reduce the effects of missing
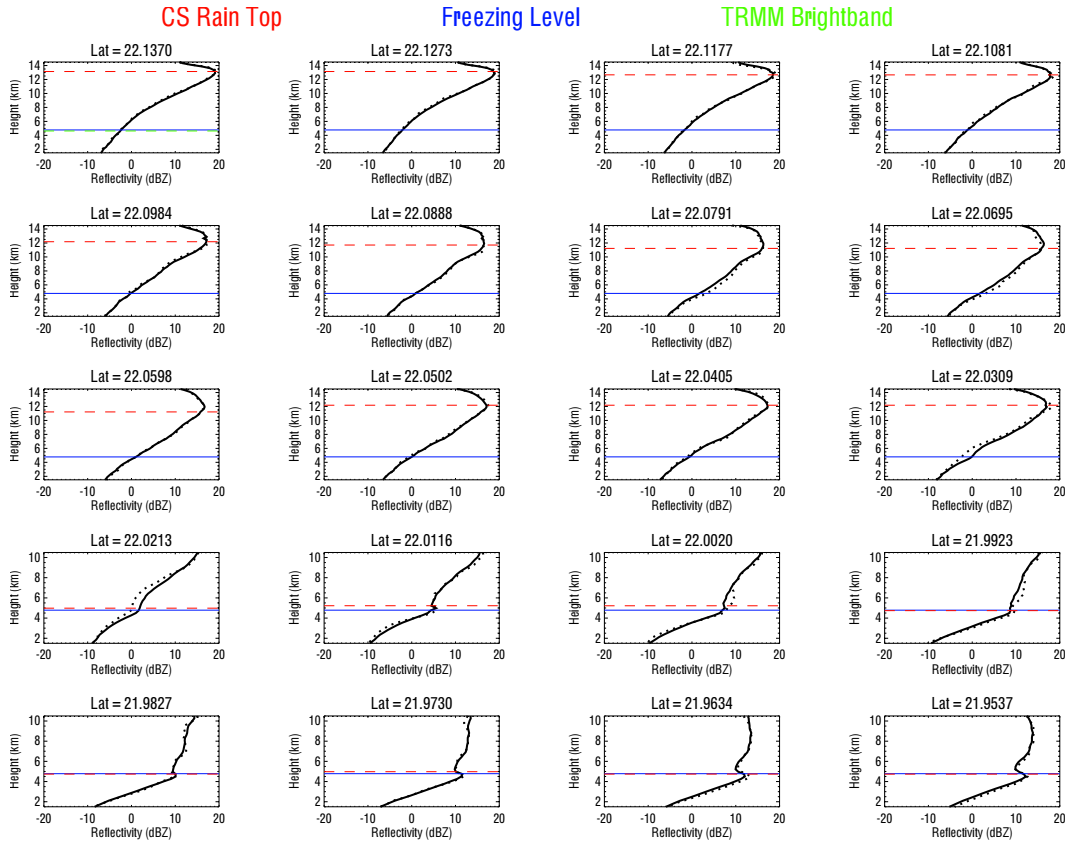
Figure 1: Example profiles demonstrating the convective/stratiform determination. The top three rows are convective profiles, while the bottom three are stratiform profiles. Blue lines indicate the freezing level, red lines the CloudSat rain top, and green lines the height of the TRMM bright band (for cases with overlap).

data, sea ice checks are only performed for profiles at locations where the monthly ice climatology suggests that sea ice is possible. When the daily data suggests sea ice is possible for the given profile or nearby profiles, the $Surface\_type$ variable is set to 7, and no precipitation rate retrieval is performed (but precipitation incidence is still evaluated).

2.2   Retrieval Flow and Diagram

A flow diagram showing the precipitation retrieval decision tree is shown in Figure 2.

3   Algorithm Inputs

3.1   CloudSat Level 2 Products

Time and location for each CloudSat pixel are supplied by the CloudSat geometric profile product (2B-GEOPROF). Table 1 summarizes the variables and their properties.
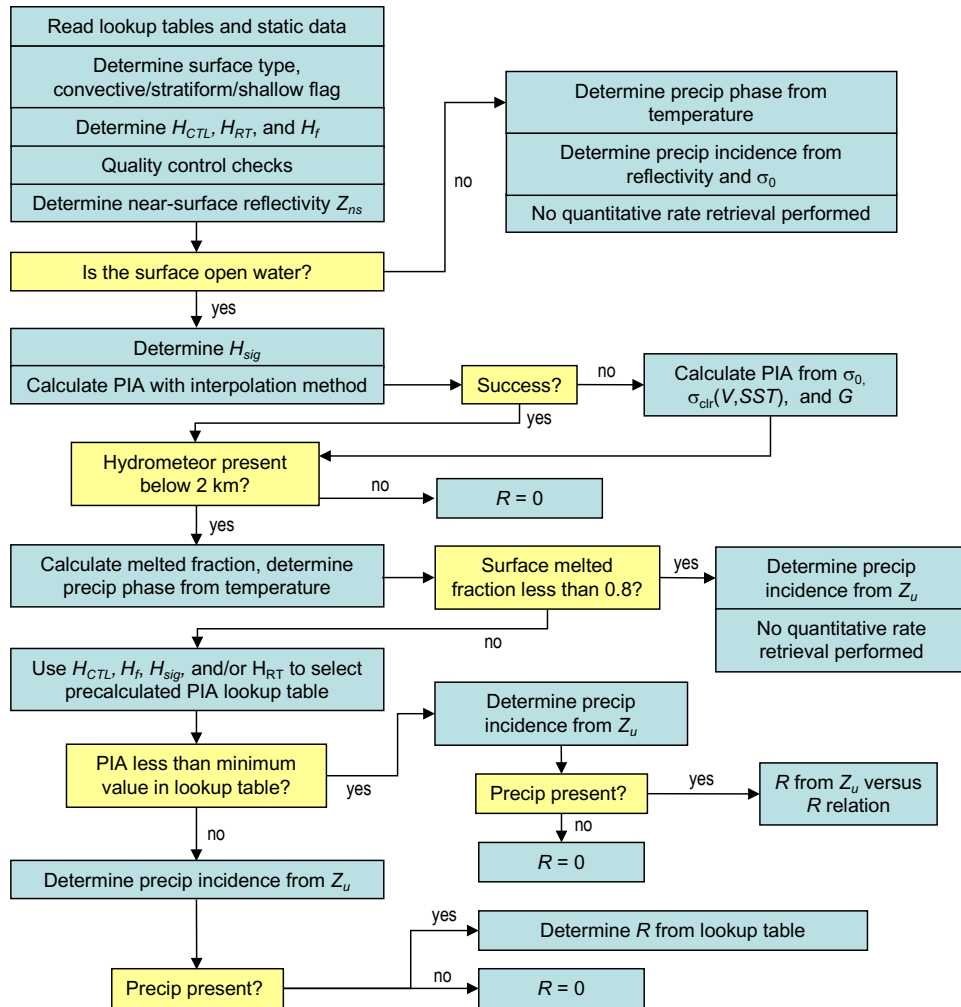
Figure 2: Flow diagram for the precipitation retrieval algorithm.

Table 1: Inputs from 2B-GEOPROF

Variable Name	Dimensions	Range	Units	Description
Per granule:				
TAI_start	scalar	$0 - 6\times10^8$	s	International Atomic Time at granule start
UTC_start	scalar	0 - 86400	s	UTC seconds since 00:00 Z of the first profile
Per profile:				
$DEM\_elevation$	scalar	-9999 - 8850	m	Elevation above mean sea level
$Profile\_time$	scalar	0 - 6000	s	Elapsed time since TAI_start
$Latitude$	scalar	-90 - +90	deg	Latitude
$Longitude$	scalar	-180 - +180	deg	Longitude
$Height$	vector (125)	-5000 - 30000	m	Height of each range bin
$Data\_quality$	scalar	0 - 127	m	Flag indicating data quality
$SurfaceHeightBin$	scalar	1 - 125	-	Bin containing surface
$SurfaceHeightBin\_fraction$	scalar	**	-	Fraction of bin to location of surface
$Navigation\_land\_sea\_flag$	scalar	1 - 3	-	Surface type characterization
$Gaseous\_Attenuation$	vector (125)	0 - 10	dBZe	Attenuation due to atmospheric gases
$Sigma\text{-}zero$	scalar	-10 - 40	dB	Normalized surface backscatter cross section
CPR_Cloud_mask	vector (125)	0 - 40	-	Cloud mask
$Radar\_reflectivity$	vector (125)	-40 to 50	dBZe	Radar reflectivity

Table 2: Inputs from ECMWF-AUX (per profile)

Variable Name	Dimensions	Range	Units	Description
$Temperature$	vector(125)	**	K	Air temperature
$Pressure$	vector(125)	**	Pa	Pressure
$Specific\_humidity$	vector(125)	**	kg/kg	Specific humidity
EC_height	vector(125)	-5000 - +30000	m	Gridbox height
$Temperature\_2m$	scalar	**	K	Two meter temperature
$U10\_velocity$	scalar	**	m s^{-1}	Zonal component of surface wind
$V10\_velocity$	scalar	**	m s^{-1}	Meridional component of surface wind
$Sea\_surface\_temperature$	scalar	**	K	Sea surface temperature

3.2   Auxiliary Data Sets

3.2.1   Numerical Model Variables

The current state of the atmosphere, including the atmospheric temperature, pressure, specific humidity, surface wind speed, and sea surface temperature are assessed from the ECMWF forecast model matched to the CPR track. Table 2 summarizes the variables and their properties.

3.2.2   Sea Ice Variables

The presence of sea ice (and inland lake ice) is determined from the daily sea ice product from SSM/I (Special Sensor Microwave Imager/Sounder) produced by the National Snow and Ice Data Center (Nolin et al. 1998). Table 3 summarizes the variables and their properties.

Table 3: Inputs from CRYOSPHERE-AUX (per profile)

Variable Name	Dimensions	Range	Units	Description
Extent	vector(49)	**	%	Sea ice concentration

3.3   Ancillary Data Sets

3.3.1   AMSR-E/AMSR2 Product Variables

The AMSR-E instrument aboard MODIS (no longer operational) and the AMSR2 instrument aboard GCOM-W1 satellite fly in formation with CloudSat. Although AMSR observations are used off-line for calibration of the σ_0 vs. V relationship, they are no longer used directly in the retrieval. Additional precipitation-related AMSR products are no longer passed through 2C-PRECIP-COLUMN, but may be found in the AMSR-AUX product.

3.4   Control and Calibration

At present no calibration of the 2C-PRECIP-COLUMN algorithm is planned. As a result, no ancillary control or calibration data is required. See Section 4.2.2 for details regarding planned validation activities for 2C-PRECIP-COLUMN products.

4   Algorithm Summary

4.1   Pseudo-code

The following provides a pseudo-code description outlining the algorithm, which is described in more detail in the algorithm flow diagram in Figure 2:

start 2C-PRECIP-COLUMN

read Input databases: Z-R, wind speed/σ_0, IGBP surface type, multiple scattering apparent attenuation

open/read/close 2B-GEOPROF, ECMWF-AUX, CRYOSPHERE-AUX

perform stratiform/convective/shallow, rain top height determination

adjust σ_0, determine its reliability

for-each profile

>   **get** height parameters (e.g. cloud base, freezing level height, height of 10 dBZ echo, rain top, significant echo height)

>   **perform** quality checks

>   **perform** incidence check over non-open water surfaces

>   **compute** PIA, near-surface PIA, and PIA uncertainty

> **compute** precip incidence from near-surface unattenuated reflectivity

> **compute** rain rate from lookup table (or Z-R relation, if needed)

end-for-each profile

open 2C-PRECIP-COLUMN output file

write output variables

close 2C-PRECIP-COLUMN output file

4.2 Algorithm Performance

4.2.1 Timing Requirements and Performance

Using a 3.1 GHz Intel Core i7 duo processor, one granule of CPR data (consisting of about 37000 rays) can be processed in approximately 94 seconds.

4.2.2 Uncertainty Requirements, Performance, and Validation

Validation of the rain incidence algorithm over ocean may be found in work by Ellis et al. (2009). This paper demonstrates that precipitation incidence from 2C-PRECIP-COLUMN is consistent with the ship-based observational climatology at lower-and-mid latitudes. At higher latitudes, 2C-PRECIP-COLUMN detects precipitation more often than other satellite based datasets (Haynes et al. 2009), which may be the result of CloudSat's higher sensitivity to frozen precipitation than existing passive sensors.

A comparison of precipitation occurrence between this product and the National Centers for Environmental Prediction (NCEP) Stage IV product, which merges WSR-88D radar data with surface rain gauge observations, may be found in Smalley et al. (2014).

5 Data Product Output

5.1 Data Format Overview

Data is provided in the HDF-EOS format. In addition to the data specific to the 2C-PRECIP-COLUMN algorithm results, the HDF-EOS data structure may incorporate granule data/metadata (describing the characteristics of the orbit or granule) and supplementary ray data/metadata. In this section, the "size" of a variable refers to a combination of the total number of profiles in a granule "nray" and the number of bytes per element (e.g., (4)). The variable type is given by REAL or INTEGER/INT (or the unsigned equivalents, UINTEGER/UINT).

5.2 Experimental Variables

Experimental output variables have names that start with "$Experimental\_$". Their use is governed by important caveats, and as such they should not be utilized without first consulting a member of the CloudSat precipitation team (see cover page).

5.3 Data Contents and Description

All of these 2C-PRECIP-COLUMN data products are summarized in Table 4 and described below.

2C-PRECIP-COLUMN Geolocation Fields:

> $Profile\_time$ (nray*REAL(4))
> > Time since TAI_start.

> UTC_start (REAL(8))
> > UTC seconds since 00:00 Z of the first profile.

> TAI_start (REAL(8))
> > International Atomic Time of first profile in granule (seconds since January 1, 1993).

> $Latitude$ (nray*REAL(4))
> > CloudSat latitude.

> $Longitude$ (nray*REAL(4))
> > CloudSat longitude.

> $DEM\_elevation$ (nray*REAL(4))
> > Elevation of surface above mean sea level; see 2B-GEOPROF documentation.

Data Fields passed through from upstream products:

> $Data\_quality$ (nray*UINTEGER(1))
> > Flag indicating data quality; see 2B-GEOPROF documentation.

> $Data\_status$ (nray*UINTEGER(2))
> > Data status flags; see 2B-GEOPROF documentation.

> $Data\_targetID$ (nray*UINTEGER(1))
> > CPR bus orientation; see 2B-GEOPROF documentation.

> $Navigation\_land\_sea\_flag$ (nray*UINTEGER(1))
> > Information on the surface type; see 2B-GEOPROF documentation.

2C-PRECIP-COLUMN Data Fields:

> $Precip\_flag$ (nray*INTEGER(1))
> > Indicates the probability precipitation is present in the profile using relative likelihood; these probabilities are segregated by the phase of the surface precipitation. (Values in Table 5)

> $Status\_flag$ (nray*INTEGER(1))
> > Indicates whether the retrieval contains only precipitation incidence information, or both incidence and intensity information. If an error condition occurred, the reason for the error is also given by this flag. (Values in Table 6)

> $Conv\_strat\_flag$ (nray*INTEGER(2))
> > Indicates whether convective, stratiform, or shallow precipitation is present. (Values in Table 7)

Table 4: Algorithm Outputs (see Section 5.3 for detailed variable descriptions)

Variable Name	Size	Range	Units	Summary Description
Geolocation Fields				
$Profile\_time$	nray*real(4)	0 - 6000	s	Elapsed time since TAI_start
UTC_start	real(4)	0 - 86400	s	UTC seconds since 00:00 Z of the first profile
TAI_start	real(8)	$0 - 6\times10^8$	s	International Atomic Time at granule start
$Latitude$	nray*real(4)	-90 - +90	deg	Latitude
$Longitude$	nray*real(4)	-180 - +180	deg	Longitude
$DEM\_elevation$	nray*real(4)	-9999 - +8850	m	Elevation of surface above mean sea level
Data Fields passed through from upstream products				
$Data\_quality$	nray*uint(1)	0 - 255	-	Flag indicating data quality
$Data\_status$	nray*uint(2)	0 - 65535	-	Data status flags
$Data\_targetID$	nray*uint(1)	0 - 203	-	CPR bus orientation
$Navigation\_land\_sea\_flag$	nray*uint(1)	1 - 5	-	Surface type characterization
Data Fields				
$Precip\_flag$	nray*int(1)	0 - 9	-	Precipitation incidence (Table 5)
$Status\_flag$	nray*int(1)	0 - 21	-	Retrieval status (Table 6)
$Conv\_strat\_flag$	nray*int(1)	-2 - +3	-	Convective/stratiform flag (Table 7)
$PIA\_hydrometeor$	nray*real(4)	-100 - +100	dB	PIA due to hydrometeors
PIA_near_sfc	nray*real(4)	-100 - +100	dB	PIA to the near-surface bin
$PIA\_uncertainty$	nray*real(4)	0 - 100	dB	PIA uncertainty
$Sigma\_zero$	nray*real(4)	-100 - +100	dB	Surface attenuated backscatter cross section
$Near\_surface\_reflectivity$	nray*real(4)	-100 - +100	dBZe	Attenuated radar reflectivity of the near-surface bin
$Frozen\_precip\_height$	nray*real(4)	0 - 20	km	Maximum height reached by frozen precipitation
$Rain\_top\_height$	nray*real(4)	0 - 18	km	Maximum height reached by liquid precipitation
$Melted\_fraction$	nray*real(4)	0 - 1	-	Mass fraction of liquid water in surface precipitation
$Lowest\_sig\_layer\_top$	nray*real(4)	0 - 20	km	Height of top of lowest significant cloud layer
$Highest\_sig\_layer\_top$	nray*real(4)	0 - 20	km	Height of top of highest significant cloud layer
$Cloud\_flag$	nray*int(1)	0 - 9	-	Cloud mask (Table 8)
$Surface\_type$	nray*int(1)	0 - 8	-	Surface type characterization
$Freezing\_level$	nray*real(4)	0 - 10	km	Height of the freezing level (ECMWF)
SST	nray*real(4)	-100 - +100	deg C	Sea surface temperature (ECMWF)
$Surface\_wind$	nray*real(4)	0 - 200	m s^{-1}	10 m wind speed (ECMWF)
$Diagnostic\_precip\_rate$	nray*real(4)	-40 - +40	mm h^{-1}	Surface precipitation rate
$Diagnostic\_precip\_rate\_min$	nray*real(4)	0 - 40	mm h^{-1}	Minimum surface precipitation rate
$Diagnostic\_precip\_rate\_max$	nray*real(4)	0 - 40	mm h^{-1}	Maximum surface precipitation rate
$Diagnostic\_precip\_rate\_no\_ms$	nray*real(4)	0 - 40	mm h^{-1}	Surface precipitation rate without M.S.
$Diagnostic\_retrieval\_info$	nray*int(1)	0 - 51	-	Additional info (Table 10)
$Diagnostic\_retrieval\_type$	nray*int(1)	0 - 9	-	Route followed by retrieval process (Table 11)
$Diagnostic\_SRT$	nray*int(1)	0 - 9	-	Surface reliability (Table 12)
$Diagnostic\_PIA\_method$	nray*int(1)	1 - 9	-	Method used to determine PIA (Table 13)
$Diagnostic\_PIA\_hydrometeor\_ws$	nray*real(4)	-100 - +100	dB	PIA using wind speed/SST method
$Diagnostic\_PIA\_uncertainty\_ws$	nray*real(4)	0 - +100	dB	PIA uncertainty using wind speed/SST method
$Experimental\_land\_PIA^*$	nray*real(4)	-100 - +100	dB	PIA due to hydrometeors over non-water surfaces
$Experimental\_land\_PIA\_uncertainty^*$	nray*real(4)	0 - 100	dB	PIA uncertainty over non-water surfaces

* If a variable name starts with "$Experimental\_$", see important usage information in Section 5.2.

$PIA\_hydrometeor$ (nray*REAL(4))

Two-way path integrated attenuation due to hydrometeors between the satellite and the surface. See $Diagnostic\_SRT$ for quality information (dB).

$PIA\_near\_surface$ (nray*REAL(4))

Two-way path integrated attenuation due to hydrometeors between the satellite and the lowest range bin the CPR can observe (dB).

$PIA\_uncertainty$ (nray*REAL(4))

Uncertainty in path integrated attenuation estimate (dB).

$Sigma\_zero$ (nray*REAL(4))

Surface attenuated backscatter cross section. See also $Diagnostic\_SRT$.

$Near\_surface\_reflectivity$ (nray*REAL(4))

Attenuated reflectivity in the fourth bin (between 600 and 840 m) above the surface.

$Frozen\_precip\_height$ (nray*REAL(4))

Estimated maximum height at which frozen precipitation is found in the column (km).

$Rain\_top\_height$ (nray*REAL(4))

Estimated maximum height at which liquid precipitation is found in the column (km).

$Melted\_fraction$ (nray*REAL(4))

The total mass fraction of liquid water contained in surface precipitation.

$Lowest\_sig\_layer\_top$ (nray*REAL(4))

The height of the top of the lowest significant cloud layer (km). A significant cloud layer is defined as one with a 2B-GEOPROF cloud mask of 30 or 40, and a reflectivity (corrected for gaseous attenuation) of at least -15 dBZ. Note that this is not necessarily a physical cloud top; use 2B-GEOPROF or 2B-GEOPROF-LIDAR to determine cloud boundaries.

$Highest\_sig\_layer\_top$ (nray*REAL(4))

The height of the top of the highest significant cloud layer (km). A significant cloud layer is defined as one with a 2B-GEOPROF cloud mask of 30 or 40, and a reflectivity (corrected for gaseous attenuation) of at least -15 dBZ. Note that this is not necessarily a physical cloud top; use 2B-GEOPROF or 2B-GEOPROF-LIDAR to determine cloud boundaries.

$Cloud\_flag$ (nray*INTEGER(1))

Indicates whether it is likely the profile is cloudy based on information from the 2B-GEOPROF cloud mask. (Values in Table 8)

$Surface\_type$ (nray*INTEGER(1))

Indicates the condition of the Earth's surface. The presence of sea ice (and inland lake ice) is determined from SSM/I (see Section 3.2.2). Since the precipitation algorithm aims to identify non-ice covered water with high confidence, the presence of ice in regions surrounding the CloudSat track can trigger an indication that sea ice or inland ice is possible. Retrievals over inland water (value of 1) should be considered experimental. (Values in Table 9)

$Freezing\_level$ (nray*REAL(4))
> The height of the freezing level; from ECMWF (km).

SST (nray*REAL(4))
> The sea surface temperature; from ECMWF (°C).

$Surface\_wind$ (nray*REAL(4))
> The surface wind speed; from ECMWF (m/s).

$Diagnostic\_precip\_rate$ (nray*REAL(4))
> Precipitation rate (mm/h). (*)
>
> If the maximum retrievable precipitation rate is encountered, $Diagnostic\_precip\_rate$ is set to a negative number. The absolute value of this number is the minimum precipitation rate for the profile; the actual precipitation rate is probably higher (and may be much higher) but can not be resolved (see discussion of the maximum retrievable precipitation rate [MRP], Haynes et al. 2009). When $Diagnostic\_precip\_rate$ is negative, $Diagnostic\_retrieval\_info$ is 50.
>
> (*) Note: This product now primarily focuses on precipitation incidence; users are directed to the 2C-RAIN-PROFILE product for quantitative rain rate information. That product considers the full radar reflectivity profile and allows precipitation rate to vary with height (unlike this product, which provides only a "column" estimate). Even so, the present product features a mature precipitation algorithm that continues to be maintained and updated, and as a service to legacy users the precipitation rate variables have been retained.

$Diagnostic\_precip\_rate\_min$ (nray*REAL(4))
> Lower bound on precipitation rate given instrument uncertainty (mm/h).

$Diagnostic\_precip\_rate\_max$ (nray*REAL(4))
> Upper bound on precipitation rate given instrument uncertainty (mm/h).

$Diagnostic\_precip\_rate\_no\_ms$ (nray*REAL(4))
> Precipitation rate that would be retrieved without considering multiple scattering effects; provided for information only, do not use as a physical precipitation rate (mm/h).

$Diagnostic\_retrieval\_info$ (nray*INTEGER(1))
> Provides additional information about the retrieval, such as the reason no precipitation intensity retrieval was preformed, and whether the precipitation was intense enough to "saturate" the surface signal (i.e. the maximum retrievable precipitation rate was encountered). (Values in Table 10)

$Diagnostic\_retrieval\_type$ (nray*INTEGER(1))
> This flag describes the route followed in the retrieval process as determined by the assumed precipitation phase. It is recommended that users use $Precip\_flag$ to determine surface precipitation type. (Values in Table 11)

$Diagnostic\_SRT$ (nray*INTEGER(1))
> Indicates the reliability of the estimate of $Sigma\_zero$ and $PIA\_hydrometeor$. Retrievals over inland water (value of 1) should be considered experimental. (Values in Table 12)

Diagnostic_PIA_method (nray*INTEGER(1))

Indicates the method used to determine $PIA\_hydrometeor$ or $Experimental\_land\_pia$ (see Section 2.1.1) (Values in Table 13)

Diagnostic_PIA_hydrometeor_ws (nray*REAL(4))

PIA using wind speed/SST method

Diagnostic_PIA_uncertainty_ws (nray*REAL(4))

Uncertainty in PIA using wind speed/SST method

Experimental_land_PIA (nray*REAL(4))

Two-way path integrated attenuation due to hydrometeors between the satellite and the surface, over non-water surfaces (dB). Experimental; see important information in Section 5.2.

Experimental_land_PIA_uncertainty (nray*REAL(4))

Uncertainty in path integrated attenuation estimate (dB). Experimental; see important information in Section 5.2.

Table 5: Values for $Precip\_flag$

Value	Meaning
0	No precip detected
9	Uncertain, see $Status\_flag$
Flags indicating surface rain	
1	Rain possible
2	Rain probable
3	Rain certain
Flags indicating surface snow	
4	Snow possible
5	Snow certain
Flags indicating surface mixed precipitation	
6	Mixed precipitation possible
7	Mixed precipitation certain

Table 6: Values for $Status\_flag$

Value	Meaning
0	Both the quantitative precip rate and occurrence retrievals were successful
1	Only the precip occurrence retrieval was successful; no precip rate was retrieved (see $Diagnostic\_retrieval\_info$)
8	No retrieval attempted (land, sea ice, unknown surface)
The following values indicate an error condition occurred:	
12	Reflectivity profile bad
13	Gaseous attenuation missing
14	SST missing
15	Surface wind speed missing
16	Sigma-zero could not be determined
17	Cloud base could not be determined
18	Near-surface reflectivity missing
19	Freezing level could not be determined
20	Non-zero $Data\_quality$ flag from 2B-GEOPROF
21	Surface bin could not be determined

Table 7: Values for $Conv\_strat\_flag$

Value	Meaning
-2	No determination possible due to shallow profile
-1	No determination possible due to bad input data
0	No certain precipitation present
1	Convective precipitation
2	Stratiform precipitation
3	Shallow precipitation

Table 8: Values for $Cloud\_flag$

Value	Meaning
0	No cloud or significant cloud not present
1	Significant cloud present with high certainty
9	Cloud presence unknown

Note: See $Lowest\_sig\_layer\_top$ in Section 5.3 for definition of what constitutes significant cloud.

Table 9: Values for $Surface\_type$

Value	Meaning
0	Open ocean (no sea ice)
1	Inland water (no ice)
7	Sea ice (or inland ice) possible
8	Land

Table 10: Values for $Diagnostic\_retrieval\_info$

Value	Meaning
0	No additional information to report
9	Uncertain, see $Status\_flag$
Reasons no quantitative precip retrieval was performed:	
1	Melted fraction of surface precipitation too small ($< 85\%$)
2	Only snow was present
8	Land, sea ice, or unknown surface
Additional information:	
3	PIA was less than the lowest table value; revert to Z-R relation
50	Precipitation rate ceiling was encountered
51	Multiple solutions were found

Table 11: Values for $Diagnostic\_retrieval\_type$

Value	Meaning
0	No precip detected
1	Rain only
2	Snow only
3	Rain and ice are present; significant stratiform precipitating ice
4	Rain and ice are present; however precipitating ice content is small and neglected in the retrieval process
5	Rain and ice are present; significant convective precipitating ice
6	The pixel is over land, sea ice, or an unknown surface, and the phase is specified exclusively in $Precip\_flag$
7	PIA was less than the lowest table value; revert to Z-R relation
9	Uncertain, see $Status\_flag$

Table 12: Values for $Diagnostic\_SRT$

Value	Meaning
0,1	$Sigma\_zero$ and $PIA\_hydrometeor$ are reliable within their estimated uncertainty range
2,3,4	$Sigma\_zero$ is NO MORE than the given value; $PIA\_hydrometeor$ is NO LESS than the given value (within uncertainty)
8	No retrieval attempted (land, sea ice, unknown surface)
9	Uncertain, see $Status\_flag$

Table 13: Values for $Diagnostic\_PIA\_method$

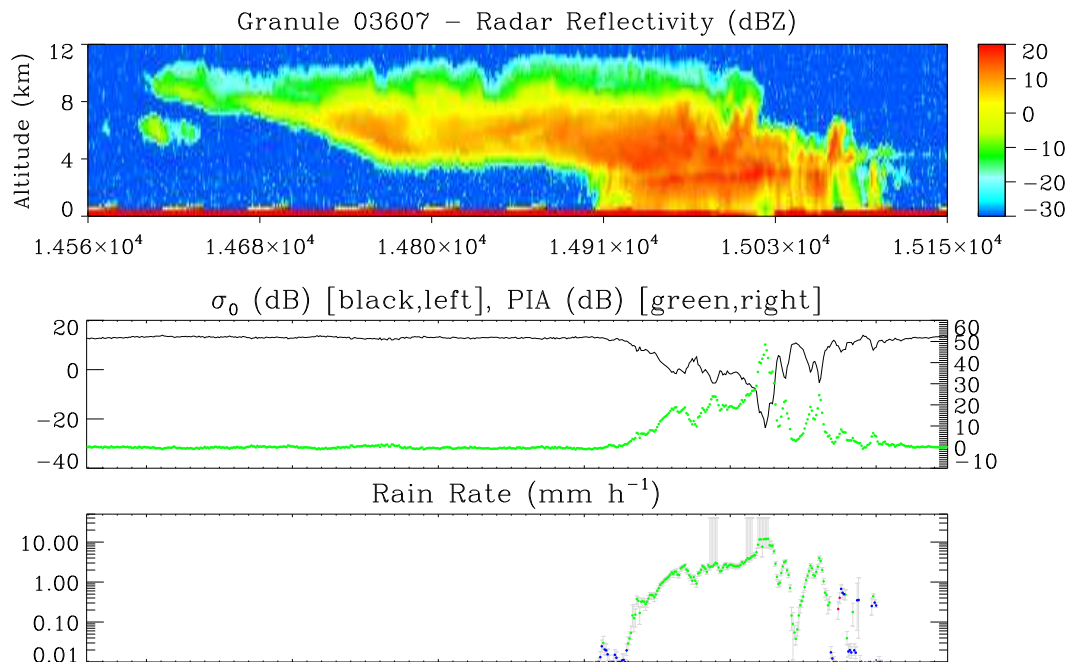| Value	Meaning
1	PIA calculated using wind speed/SST method
2	PIA calculated using interpolation method
3	PIA calculation failed
9	Uncertain, see $Status\_flag$

6 Example

Figure 3: Sample retrieval for granule 3607, profiles 14560 through 15150. Top panel shows radar reflectivity profile. Middle panel shows σ_0 (black line, left scale) and PIA to the surface (green dots, right scale). Bottom panel shows retrieved rain rate (colored dots) and uncertainties (bars). Green dots: "rain certain"; blue dots: "rain probable"; red dots: "rain possible." (Version P1_R05 shown.)

An example of a rain retrieval over a 645 km swath of mostly stratiform precipitation in the Southern Pacific observed by the CPR on 2007 January 1 is shown in Figure 3. The freezing level in this case is near 3.3 km. The middle panel demonstrates that σ_0 is correlated with the strength of the surface reflectivity. In the heavy raining core near profile 15025, for example, σ_0 drops to approximately -38 dB. The calculated PIA peaks near 48 dB. Retrieved surface rain rates are shown in the bottom panel, with bars indicating the calculated uncertainties associated with the PIA measurement. While rain rates are generally a few mm/h or lighter, in several locations the MRP is reached and the upper bound on rain rate can not be determined. The colored dots correspond to varying likelihood that rain is actually occurring at the surface.

7 Operator Instructions

The 2C-PRECIP-COLUMN product processing software is part of the CloudSat Operational and Research Environment (CORE). Standard CORE modules for operating on data files are utilized.

8   Acronym List

AMSR-E Advanced Microwave Scanning Radiometer for EOS

AMSR2 Advanced Microwave Scanning Radiometer 2

CORE CloudSat Operational and Research Environment

CPR Cloud Profiling Radar

ECMWF European Centre for Medium-Range Weather Forecasts

EOS Earth Observing System

HDF Hierarchical Data Format

IGBP International Geosphere-Biosphere Programme

MRP Maximum Retrievable Precipitation Rate

NCEP National Centers for Environmental Prediction

PIA Path Integrated Attenuation

SST Sea Surface Temperature

TRMM Tropical Rainfall Measurement Mission

WSR-88D Weather Surveillance Radar, 1988 Doppler

References

Battaglia, A., M. O. Ajewole, and C. Simmer, 2007: Evaluation of radar multiple scattering effects in cloudsat configuration. *Atmos. Chem. Phys.*, **7**, 1719-1730.

Ellis, T. D., T. L'Ecuyer, J. M. Haynes, and G. L. Stephens, 2009: How often does it rain over the global oceans? The perspective from CloudSat. *Geophys. Res. Lett.*, **36**, L03815, doi:10.1029/2008GL036728.

Haynes, J. M., T. S. L'Ecuyer, G. L. Stephens, S. D. Miller, C. Mitrescu, N. B. Wood, and S. Tanelli, 2009: Rainfall retrieval over the ocean with spaceborne W-band radar. *J. Geophys. Res.*, **114**, D00A22, doi:10.1029/2008JD009973.

Hogan, R. J., and A. Battaglia, 2008: Fast lidar and radar multiple-scattering models. Part II: Wide-angle scattering using the time-dependent two-stream approximation. *J. Atmos. Sci.*, **65**, 3636-3651.

Li, L., G. M. Heymsfield, L. Tian, and P. E. Racette, 2005: Measurements of ocean surface backscattering using an airborne 94-GHz cloud radar - Implication for calibration of airborne and spaceborne W-Band radars. *J. of Atmos. and Oceanic Technol.*, **22**, 1033-1045.

Nolin, A., R. L. Armstrong, and J. Maslanik, 1998: Near-Real-Time SSM/I-SSMIS EASE-Grid Daily Global Ice Concentration and Snow Extent, Version 2, Boulder, Colorado USA: National Snow and Ice Data Center.

Smalley, M., T. L'Ecuyer, M. Lebsock, and J. Haynes, 2014: A comparison of precipitation occurrence from the NCEP Stage IV QPE product and the CloudSat Cloud Profiling Radar. *J. Hydrometeor*, **15**, 444-458.

Wallace, J. M., and P. V. Hobbs, 2006: *Atmospheric science: An introductory survey*. 2nd ed. Elsevier Academic Press, Amsterdam.